J Biol Chem. 2010 January 29; 285(5): 3133–3144.
Published online 2009 November 24. doi: 10.1074/jbc.M109.077271
PMCID: PMC2823454

Exogenous NAD Blocks Cardiac Hypertrophic Response via Activation of the SIRT3-LKB1-AMP-activated Kinase Pathway*

Vinodkumar B. Pillai,[‡] Nagalingam R. Sundaresan,[‡] Gene Kim,[§] Madhu Gupta,[¶] Senthilkumar B. Rajamohan,[‡] Jyothish B. Pillai,[‡] Sadhana Samant,[‡] P. V. Ravindra,[‡] Ayman Isbatan,[‡] and Mahesh P. Gupta[‡▫1]

From the Departments of [‡]Surgery and
[§]Medicine and
[▫]Committee on Cellular and Molecular Physiology, Biological Science Division, University of Chicago, Chicago, Illinois 60637 and
the [¶]Department of Physiology and Biophysics, University of Illinois, Chicago, Illinois 60612
[1] To whom correspondence should be addressed: Dept. of Surgery, University of Chicago, 5841 S. Maryland Ave., Chicago, IL 60637., E-mail: mgupta@surgery.bsd.uchicago.edu .

Received October 19, 2009; Revised November 23, 2009

Abstract

Since the discovery of NAD-dependent deacetylases, sirtuins, it has been recognized that maintaining intracellular levels of NAD is crucial for the management of stress response of cells. Here we show that agonist-induced cardiac hypertrophy is associated with loss of intracellular levels of NAD, but not exercise-induced physiologic hypertrophy. Exogenous addition of NAD was capable of maintaining intracellular levels of NAD and blocking the agonist-induced cardiac hypertrophic response *in vitro* as well as *in vivo*. NAD treatment blocked the activation of pro-hypertrophic Akt1 signaling, and augmented the activity of anti-hypertrophic LKB1-AMPK signaling in the heart, which prevented subsequent induction of mTOR-mediated protein synthesis. By using gene knock-out and transgenic mouse models of SIRT3 and SIRT1, we showed that the anti-hypertrophic effects of exogenous NAD are mediated through activation of SIRT3, but not SIRT1. SIRT3 deacetylates and activates LKB1, thus augmenting the activity of the LKB1-AMPK pathway. These results reveal a novel role of NAD as an inhibitor of cardiac hypertrophic signaling, and suggest that prevention of NAD depletion may be critical in the treatment of cardiac hypertrophy and heart failure.

Keywords: AMP-activated Kinase (AMPK), Heart, Histone Deacetylase, Oxidative Stress, Signal Transduction, AMPK Signaling, Cardiac Hypertrophy, Heart Failure, Histone Deacetylases, Sirtuins

Introduction

Cardiac hypertrophy is a complex growth response of the heart, whereby terminally differentiated cardiac myocytes structurally, genetically, and functionally remodel in response to a variety of physiologic and pathologic stimuli. In settings of pathologic stimuli, such as hypertension, ischemic disease, or valvular insufficiency, cardiac hypertrophy develops with enlarged cardiomyocytes, which are associated with formation of new sarcomeres and induction of a group of genes (fetal genes), which are usually expressed during development of the fetal heart. These changes provide a short term mechanism for decreasing ventricular wall stress and improving heart function. However, during prolonged intervals of pathologic hypertrophy, this program becomes maladaptive, resulting in myocyte cell death, fibrosis, and ventricular dilation and the transition to heart failure (1). Recent evidence suggests that reduction of cardiac hypertrophy

could block the onset of heart failure and improve patient survival (1,–3). One novel approach that is gaining increasing attention in this direction is the activation of endogenous cell signaling pathways that negatively regulate cardiac hypertrophy (4). Exogenous agents that can facilitate the activity of these pathways are of particular interest as new therapeutic tools for the management of cardiac hypertrophy and heart failure.

At the cellular level various signaling mechanisms have been described that lead to development of cardiac hypertrophy. Among them, oxidative stress is recognized as a critical common signal to various stimuli, which directs to evolution of pathologic hypertrophy (5). Severe oxidative stress can result in increased NAD turnover due to increased activity of NAD-consuming enzymes such as poly(ADP-ribose) polymerase-1 and/or decreased activity of NAD salvage pathways, with a net result of depletion of intracellular NAD levels (6). Loss of NAD can make a cell unable to carry out its energy-dependent functions and defend itself against oxidative stress because of loss of activity of certain cell-survival factors that are NAD-dependent, such as sirtuins.

Sirtuins are class III HDACs,[2] which are expressed as seven different (SIRT1–SIRT7) isoforms in mammals. They are considered to be key regulators of many cellular functions, including stress resistance, energy metabolism, apoptosis, and aging (7). Increased activity of the prototype member of this family, SIRT1, has been shown to protect cardiomyocytes from oxidative stress-mediated cell death and retard certain cardiac degenerative changes associated with aging. However, these cardioprotective effects of SIRT1 were seen only at low dosage, but not at a high dosage of SIRT1. In fact, overexpression of SIRT1 in mouse hearts was shown to produce hypertrophic cardiomyopathy associated with ATP depletion and reduced expression of citrate synthase and peroxisome proliferator-activated receptor-γ co-activator 1α, an indication of impaired mitochondrial function and density (8).

Another sirtuin analogue, SIRT3, has been shown to be highly expressed in the heart and it is activated during cardiomyocytes stress. Increased activity of SIRT3 protects cardiomyocytes from oxidative stress-mediated cell death by increased expression of antioxidants, Mn-SOD and catalase (9). SIRT3 has been also shown to preserve the ATP biosynthetic capacity of the heart (10). Among different sirtuin analogues, *SIRT3* is the only analogue that has been implicated in extension of the lifespan of humans. The polymorphism in the *SIRT3* promoter, which renders gene activation, was found to be associated with human longevity (11, 12). A recent study has shown that SIRT3 levels are reduced in older patients (65 plus years) with a sedentary lifestyle and are elevated after endurance exercise, which delayed signs of senescence, thus suggesting a role of SIRT3 in counteracting the aging process in humans (13). However, chemical agents that could elevate cellular levels of SIRT3, without inducing cellular stress, have not yet been identified. Previous studies have shown that the intracellular NAD/NADH ratio regulates the levels of sirtuins, including SIRT3 and SIRT1 (14). Although high levels of NAD up-regulate the levels of sirtuins, high levels of NADH and nicotinamide do the opposite. A recent report has indicated that exogenous NAD can enter the neurons and protect them from degeneration and ischemia-induced cell death (15). It is therefore likely that by maintaining an adequate intracellular level of NAD, cardiomyocytes could be also protected from hypertrophy and cell death by increasing the activity of one or more sirtuin analogues.

In this study we report that pathologic cardiac hypertrophy is associated with depletion of cellular NAD levels. Exogenous supplementation of NAD restores the intracellular levels of NAD and blocks the cardiac hypertrophic response. We also demonstrate that anti-hypertrophic effects of NAD are mediated via activation of SIRT3, but not SIRT1. The experiments performed to delineate the downsteam mechanism of NAD-mediated cardiac protection demonstrated that exogenous NAD restored the activity of endogenous anti-hypertrophic signaling via activation of the SIRT3-LKB1-AMPK pathway. To the best of our knowledge, this report represents the first application of NAD in the treatment of cardiac hypertrophy.

MATERIALS AND METHODS

Induction of Hypertrophy in Mice

Angiotensin-II or isoproterenol were dissolved in 150 mM NaCl and 1 mM acetic acid. Angiotensin-II was delivered chronically at a rate of 3.0 mg/kg/day for 14 days. Isoproterenol was infused at a rate of 8.7 mg/kg/day for 7 days by implanting osmotic mini-pumps (ALZET model 2002) in the peritoneal cavity of mice. Control mice underwent the same procedure, except that the respective pumps were filled only with vehicle (150 mM NaCl, 1 mM acetic acid). Exogenous NAD was given at the rate of 1 mg/kg/day for the entire duration of treatment with the hypertrophy agonist. Physiologic hypertrophy was induced by subjecting the mice to swimming for 12 weeks at 1-h/day for 5 days a week.

Primary Cultures of Cardiomyocytes, Transfection/Infection, and Luciferase Assay

Neonatal rat cardiomyocytes were cultured and infected with adenoviral vectors as described earlier (16). *NFAT*-luciferase, *CARP*-luciferase, and *ANF*-luciferase vector contains multiple binding sites for *NFAT*, *CARP*, and *ANF*, respectively. Cells were transfected with the use of Tfx-20 (Promega) reagent as per the manufacturer's protocol. A luciferase activity assay was performed by use of the luciferase activity assay kit from Promega according to the manufacturer's protocol. Values were normalized with the protein content of the cell.

Reactive Oxygen Species (ROS) Detection

ROS were detected using CM-H_2DCFDA (Invitrogen) as per the manufacturer's instructions. Briefly, primary cultures of cardiomyocytes were treated with 20 μM phenylephrine (PE) in the presence or absence of 250 μM NAD for 15 min. Cells were stained with CM-H_2DCFDA. Cells were acquired by FACSCalibur and analyzed with FlowJo. The mean fluorescence intensity of cells positive for CM-H_2DCFDA staining was determined.

Histology and Immunohistochemistry

For detection of cell size, heart sections were stained with wheat germ agglutinin coupled to tetramethylrhodamine isothiocynate (Sigma). The cell size of myocytes was measured by use of NIH ImageJ software. Fibrosis was detected with use of Masson's trichrome staining kit from Sigma according to the manufacturer's protocol. ANF release from nuclei of cardiomyocytes was determined by staining the cells with antibodies specific for α-actinin and ANF.

Real Time PCR Analysis of mRNA Levels

The mRNA levels of *ANF*, brain natiuretic peptide, β-myosin heavy chain, and *Collagen*-α were measured by SYBR Green real time PCR as per the protocol described earlier (17). Total RNA was isolated from mouse hearts using TRIzol reagent (Invitrogen). The residual genomic DNA was digested by incubating the RNA preparation with 0.5 units of RNase-free DNase I/μg of RNA in 1× reaction buffer for 15 min at room temperature, followed by heat inactivation at 90 °C for 5 min. The quality of DNase I-treated RNA was tested by formaldehyde-agarose gel electrophoresis. Two micrograms of DNase I-treated RNA was reverse transcribed by use of the Superscript III (Invitrogen). The resultant cDNA was diluted 10-fold prior to PCR amplification. A reverse transcriptase minus reaction served as a negative control.

[^{3}H]Leucine Incorporation

Immediately after treatment of cardiomyocytes with PE, cells were incubated with [^{3}H]leucine (1.0 mCi/ml, 163 Ci/mmol specific activity, Amersham Biosciences) in leucine-free minimal essential medium (Invitrogen) for 48 h. Cells were washed with phosphate-buffered saline and then incubated in 10% trichloroacetic acid to precipitate proteins. The resultant pellet was solubilized in 0.2 N NaOH and diluted with one-sixth volume of scintillation fluid and counted in a scintillation counter. Values were normalized with DNA content, which was measured by use of Quant-iT picogreen double-stranded DNA assay kit (Invitrogen).

Antibodies

SIRT3 and phospho-mTOR (Ser-2446) antibodies were from Abgent, SIRT1 antibody was from Millipore, LKB1 was from Sigma, and Nampt antibody from Alexis, Inc. All other antibodies were purchased from Cell

Signaling Inc.

NAD and ATP Estimation

The NAD levels were measured according to the method described previously by Jacobson and Jacobson (18) with a slight modification. An average of 1×10^5 cells or 50 mg of frozen crushed tissue was suspended in 200 μl of 0.5 M perchloric acid. The cell extract was neutralized with an equal volume of 1 M KOH and 0.33 M KH_2PO_4/K_2HPO_4 (pH 7.5) and centrifuged to collect the supernatant and remove the $KClO_4$ precipitate. The supernatant (50 μl; or NAD standard) was added to 200 μl of NAD reaction mixture (600 mM ethanol, 0.5 mM 3-(4,5-dimethylthiazol-2-yl)-2,5-diphenyltetrazolium bromide, 2 mM phenazine ethosulfate, 5 mM EDTA, 1 mg/ml of bovine serum albumin, and 120 mM Bicine, pH 7.8) and incubated for 5 min at 37 °C. The reaction was initiated by the addition of 25 μl of alcohol dehydrogenase (0.5 mg/ml in 100 mM Bicine, pH 7.8) and incubated for 20 min at 37 °C, and stopped by addition of 250 μl of 12 mM iodoacetate. The absorbance of the reaction mixture was read at a wavelength of 570 nm. The NAD content was measured from the standard curve and normalized to the protein content of the sample. The cellular ATP levels were measured using a bioluminescence assay kit (Roche Applied Science). Cells (1×10^5) or frozen crushed tissue (50 mg) were lysed in 200 μl of cell lysis reagent (Roche Applied Science). Luciferase reagent (100 μl) and dilution buffer (50 μl) were added to 50 μl of lysate, and luminescence was analyzed after a 1-s delay with a 10-s integration on a luminometer. A standard curve was generated from known amounts of ATP and used to calculate the ATP content of the sample. Values were normalized to the total protein content of the sample.

Sirt1$^{-/-}$, Sirt3$^{-/-}$, and Sirt3 Transgenic Mice

Sirt3 and *Sirt1* knock-out mice were generously provided by F. W. Alt and M. W. McBurney, respectively. All experiments with *Sirt3* transgenic mice, except *in vivo* interaction of *Sirt3* with LKB1, were performed using transgenic mice expressing the short form of SIRT3 (9). For studying *in vivo* interaction of SIRT3 with LKB1, *Sirt3* transgenic mice expressing the long form of *Sirt3* with the C-terminal hemagglutinin tag was utilized. These transgenic mice were generated and characterized similar to the method described earlier (9).

In Vitro Acetylation Assay

Immunoprecipitated LKB1 bound to beads were incubated with 200 ng of active PCAF (or P300) enzyme (Upstate Biotechnology), 0.5 mM acetyl-CoA (Sigma), 50 mM nicotinamide, and 10 μM trichostatin in 1× HAT buffer (50 mM Tris, pH 8.0, 10% glycerol, 0.1 mM EDTA, 1 mM dithiothreitol) for 30 min at 30 °C on a rotator. Unacetylated LKB1 contained all components except acetyl-CoA. Reactions were terminated by adding SDS sample buffer and resolved on a 10% SDS-polyacrylamide gel. Proteins were transferred to a Hybond-P membrane (GE Healthcare) and detected by Western analysis with anti-Ac-K antibody.

In Vitro Deacetylation Assay

Immunoprecipitated and *in vitro* acetylated LKB1 bound to beads was resuspended in 1× HDAC buffer (25 mM Tris/Cl, pH 8.0, 137 mM NaCl, 2.7 mM KCl, 1 mM $MgCl_2$, and 0.1 mg/ml of bovine serum albumin). For SIRT3-mediated deacetylation, 40 ng/μl of SIRT3 (catalytic domain, Abcam, Inc.) was added to HDAC buffer in the presence or absence of 500 μM NAD. The reaction mixture was incubated for 1 h at 30 °C on a nutator. Proteins were resolved by SDS-PAGE and analyzed by either autoradiography or Western blotting with anti-Ac-K antibody.

Echocardiography of Mice

Chest hair of mice were removed with a topical depilatory agent and transthoracic echocardiography was performed under inhaled isoflurane (~1%) for anesthesia, delivered via nose cone. Limb leads were attached for electrocardiogram gating, and the animals were imaged in the left lateral decubitus position with a VisualSonics Vevo 770 machine, using a 30 MHz high frequency transducer. Body temperature was maintained using a heated imaging platform and warming lamps. Two-dimensional images were recorded in parasternal long- and short-axis projections, with guided M-mode recordings at the midventricular level in

both views. LV (left ventricle) cavity size and wall thickness were measured in at least 3 beats from each projection and averaged. LV wall thickness (interventricular septum and posterior wall thickness) and internal dimensions at diastole and systole (LVIDd and LVIDs, respectively) were measured. LV fractional shortening ([LVIDd − LVIDs]/LVIDd) and relative wall thickness ([interventricular septum thickness + posterior wall thickness]/LVIDd) were calculated from M-mode measurements.

Statistical Analysis

Student's paired two-tailed test was applied to determine statistical significance between two groups. *p* values less than 0.05 was considered significant.

RESULTS

NAD Treatment Protects Cardiomyocytes from Agonist-mediated Hypertrophy

Mounting evidence has indicated that induction of ROS is necessary for the development of cardiomyocyte hypertrophy (5, 9, 19, 20). Therefore, to test the cardioprotective effects of NAD, we first examined the ability of NAD to block agonist-induced ROS production of cardiomyocytes. Cultures of cardiomyocytes were treated with PE, a hypertrophy agonist, in the presence or absence of NAD. Cells were stained with CM-H_2DCFDA, a non-fluorescent dye that fluoresces by ROS-mediated removal of an acetate group by intracellular esterases. We found that NAD treatment suppressed the PE-induced mean fluorescence intensity of the dye to a level that was comparable with control cells, thus suggesting that NAD treatment was capable of blocking the PE-induced ROS synthesis of cardiomyocytes (Fig. 1).

These data also indicated that hypertrophy of cardiomyocytes may result from loss of cellular NAD levels, and if so, then supplementation of NAD should be able to rescue cells from developing hypertrophy. To test this hypothesis, we treated cardiomyocytes with PE (20 μM), or PE treatment was given together with NAD (250 μM). The results showed that PE treatment caused depletion of cellular NAD levels by nearly 25%, and exogenous addition of NAD was capable of rescuing cells from this NAD loss. A corresponding depletion of ATP was also observed, which was again rescued by NAD treatment (Fig. 2, *A* and *B*). To examine the effect of NAD on hypertrophy of cardiomyocytes, we stimulated cells with PE (20 μM) or angiotensin-II (Ang-II) (2 μM), another hypertrophy agonist, in the presence or absence of NAD (250 μM). The hypertrophic response of cells was measured by increased protein synthesis as determined by increased [^{3}H]leucine incorporation into total cellular proteins and by release of ANF from nuclei, a hallmark of cardiac hypertrophy. We found significantly higher [^{3}H]leucine incorporation in PE- and Ang-II-treated cardiomyocytes compared with controls. Addition of NAD to cultures prevented this agonist-mediated increased leucine incorporation into proteins (Fig. 2*C*). Similarly, NAD treatment also blocked the induction of ANF release from nuclei, thus suggesting the anti-hypertrophic activity of NAD (Fig. 2*D*). To confirm these results, we examined the effect of NAD on the promoter activity of three hypertrophy signal-sensitive genes, *ANF*, *CARP*, and *NFAT*. The results indicated that PE-mediated activation of these promoters was significantly reduced by treatment of cells with NAD, thus again demonstrating the anti-hypertrophic potential of NAD (Fig. 2, *E–G*). We next asked how NAD enters into cardiomyocytes. Bruzzone *et al.* (21) have shown that connexin 43 (Cx43) channels are permeable to extracellular NAD. Because cardiomyocytes express a large amount of Cx43 channels, we tested the effect of exogenous NAD in the presence of a Cx43 channel blocker, carbenoxolone. The results showed that in the presence carbenoxolone NAD treatment failed to block agonist-induced ANF release from nuclei, thus demonstrating that exogenous NAD is likely to enter into cardiomyocytes via the Cx43 channels (Fig. 2*D*).

NAD Treatment Blocks Agonist-induced Cardiac Hypertrophy in Vivo

To determine the ability of NAD to block the hypertrophic response of hearts *in vivo*, we infused mice with Ang-II for 2 weeks. Mice were simultaneously treated with NAD at 1 mg/kg/day for 2 weeks, or with the vehicle. Ang-II infusion in control mice produced nearly 25% cardiac hypertrophy, which was associated with

increased size of myocytes and accumulation of fibrosis in the interstitial space. These changes were markedly reduced by treatment of mice with NAD (Fig. 3, *A*–*D*). Ang-II infusion also significantly induced the expression of *ANF*, brain natiuretic peptide, β-myosin heavy chain, and *Collagen*-α mRNAs in the control hearts. Expression levels of these markers was also dramatically reduced by NAD treatment of the mice, thus suggesting that NAD treatment has the capacity to block Ang-II-mediated cardiac hypertrophy *in vivo* (Fig. 3, *E* and *F*). We also measured the NAD and ATP levels in these hearts, and we found that, whereas NAD levels were reduced by nearly 28% in Ang-II-infused hearts, they were generally maintained at control levels in NAD-treated hearts (Fig. 3*G*). Similar changes were noted for ATP levels of NAD-treated and untreated hearts (Fig. 3*H*). Thus, consistent with our *in vitro* results, these data demonstrated that NAD treatment was capable of maintaining cellular NAD levels and blocking the cardiac hypertrophic response.

Knowing that maintenance of intracellular levels of NAD prevents development of agonist-induced hypertrophy, we then measured NAD levels in hearts of mice subjected to swim-induced physiologic hypertrophy. The results showed that, unlike Ang-II-infused hearts, no NAD loss was detected in hearts of mice having exercise-induced physiologic hypertrophy, thus suggesting that depletion of cellular NAD levels is in fact a characteristic of pathologic cardiac hypertrophic response (Fig. 3, *G* and *H*).

NAD Treatment Blocks Cardiac Hypertrophy via Activation of the LKB1-AMPK Signaling Pathway

In skeletal muscle cells, increased intracellular levels of NAD were shown to activate AMPKα (hereafter referred as AMPK) (22). Activation of AMPK has also been implicated in limiting the cardiac hypertrophic response (23). We therefore focused our attention on the involvement of the AMPK signaling pathway in NAD-mediated cardiac protection. The results showed that AMPK activation (phosphorylation) was reduced substantially in PE-stimulated cells, but not when PE stimulation was given together with NAD (Fig. 4*A*). The activity of AMPK is known to be regulated by an upstream kinase, LKB1 (24). We therefore examined phosphorylation of LKB1, and found that, just as for AMPK, LKB1 phosphorylation was also substantially reduced in PE-stimulated cardiomyocytes, but again not when cells were treated with NAD, thus suggesting that NAD treatment had the capacity to protect the activity of LKB1 and AMPK.

We then examined the downstream targets of AMPK that are involved in the development of cardiomyocyte hypertrophy. mTOR and GSK3β are two key enzymes that participate in the evolution of cardiac hypertrophy (25). Whereas increased activity of mTOR promotes induction of hypertrophy, activation of GSK3β does the opposite (25). The activity of mTOR is regulated by Raptor, a target of AMPK. AMPK phosphorylates Raptor at Ser-792, which promotes its ability to bind to mTOR, resulting in inhibition of mTOR (26). AMPK also directly inhibits mTOR by phosphorylating mTOR at Thr-2446 (27), thereby blocking its pro-hypertrophic activity. We found that phosphorylation of Raptor (Ser-792) and mTOR (Thr-2446) was reduced in PE-stimulated cells, whereas it was maintained at control levels in NAD-treated cardiomyocytes (Fig. 4*A*).

AMPK activation is also known to negatively regulate the activity of PKB/Akt1 (23, 27), an upstream kinase of both mTOR and GSK3β. Contrary to the finding for AMPK, we found increased phosphorylation of Akt1 and GSK3β in PE-stimulated cells, but not in NAD-treated cells (Fig. 4*A*). In this experiment, we also found increased phosphorylation of extracellular signal-regulated kinase (ERK) 1/2 in PE-stimulated cells, which was again restored to control levels after NAD treatment (Fig. 4*A*). These results indicated that NAD treatment prevented the development of cardiomyocyte hypertrophy via activation of the inherent anti-hypertrophic mechanism by augmenting the activity of the AMPK signaling pathway.

We then asked whether the signaling mechanism operating *in vitro* can be recapitulated in *in vivo* models of cardiac hypertrophy. The results showed that, same as *in vitro*, Ang-II-stimulated hypertrophied hearts had decreased phosphorylation of AMPK, LKB1, Raptor, and mTOR (Thr-2446), and increased phosphorylation of Akt1 and GSK3β (Fig. 4*B*). Akt1 is known to phosphorylate mTOR at Ser-2448, which (unlike Thr-2446 phosphorylation) increases the activity of mTOR and thereby enhances its capacity to promote protein

synthesis by activating the downstream kinases that phosphorylate ribosomal proteins. In accordance with Akt1 activation, we found increased phosphorylation of mTOR at Ser-2448 and S6 ribosomal protein during Ang-II-induced hypertrophy of the heart. The activity of all of these targets of AMPK and Akt1 was restored to control levels after NAD treatment of mice (Fig. 4*B*). We, however, found no change in the activity of p38 in these hearts, which served as a negative control.

Because in our earlier experiments we found no change in intracellular levels of NAD during physiologic hypertrophy, we wondered whether the activity of AMPK was maintained in these hearts. The results indicated that unlike Ang-II-stimulated hearts, the activity of AMPK and LKB1 in hearts of mice subjected to swim exercise was increased compared with controls (Fig. 4*C*). These data thus confirmed that maintenance of intracellular levels of NAD blocked the agonist-induced pathologic hypertrophic response in part, by activation of LKB1-AMPK signaling pathway.

The Anti-hypertrophic Effect of NAD Is Mediated via Activation of SIRT3, but Not SIRT1

Knowing that NAD protected the activity of LKB1 and AMPK, we next explored the upstream activator of these kinases. AMPK has been shown to activate the key enzyme of the NAD-salvage pathway, Nampt (nicotinamide phosphoribosyltransferase) (22). We therefore asked whether the activity of Nampt was also reduced during pathologic hypertrophy. The results indicated that this was indeed the case. Decreased levels of phospho-AMPK were accompanied with decreased levels of Nampt in hypertrophied hearts, and NAD treatment rescued both of them to control levels (Fig. 4*B*).

Increased cellular levels of Nampt and NAD are known to enhance the activity of SIRT1 (28). SIRT1 has been shown to deacetylate LKB1 in human embryonic kidney 293 cells, resulting in activation (phosphorylation) of the kinase (29). Based on this information, we posited that the anti-hypertrophic effects of NAD could be mediated by sequential activation of SIRT1, LKB1, and AMPK. To test this hypothesis, we examined the acetylation (which corresponds with deactivation/dephosphorylation of the enzyme) of LKB1 in hearts of mice of different groups. We found increased acetylation of LKB1 during Ang-II-mediated cardiac hypertrophy, which was reduced substantially after NAD treatment (Fig. 5*A*). To test whether SIRT1 was indeed involved in NAD-mediated deacetylation (activation) of LKB1, we examined the phosphorylation of LKB1 and AMPK in *Sirt1*$^{-/-}$ mice. To our surprise, we found increased phosphorylation of both LKB1 and AMPK in *Sirt1*$^{-/-}$ hearts, thus suggesting that the activation of these kinases was not regulated by SIRT1 in the heart (Fig. 5*B*). This raised questions for the participation of SIRT1 in the cardioprotective effects of NAD. To confirm these results, we then examined the anti-hypertrophic effect of NAD in *Sirt1*$^{+/-}$ mice (*Sirt1*$^{-/-}$ mice rarely survive beyond a few days after birth). For this experiment, animals were infused with isoproterenol (ISO), another potent agonist of pathologic cardiac hypertrophy. The results showed a robust hypertrophic response of SIRT1$^{+/-}$ mice to ISO infusion, which was again blocked by NAD treatment of mice, suggesting that SIRT1 was not entirely needed for the anti-hypertrophic effects of NAD (Fig. 5, *C–E* and *G*).

To get additional evidence for these findings, we examined the effect of *in vitro* NAD treatment in the presence of splitomicin, a SIRT1 inhibitor (30). We also examined the effect of compound C, a AMPK inhibitor (31) to obtain further support for the involvement of AMPK in NAD-mediated cardiac protection. Cells were pretreated with splitomicin or compound C and then stimulated with PE, either alone or together with NAD. The hypertrophic response of cardiomyocytes was examined by measuring [^{3}H]leucine incorporation into total cellular protein. The results showed that pretreatment of cells with compound C, but not splitomicin, eliminated the anti-hypertrophic effect of NAD (Fig. 5*H*). These data taken together indicate that the anti-hypertrophic effect of exogenous NAD was not dependent on SIRT1, but required AMPK.

Besides SIRT1, no other sirtuin has been shown so far to activate LKB1 and AMPK. Because LKB1 was deacetylated in NAD-treated hearts, it indicated that there must be another analogue of sirtuins, which has the capacity to deacetylate and activate LKB1 in the heart. To identify this new activator of LKB1 we tested

expression levels of different members of the sirtuin family in hypertrophied hearts treated with NAD. We found that cardiac SIRT3 levels were highly elevated after NAD treatment of mice (Fig. 6*A*). We then determined the role of SIRT3 in activation of LKB1. To this end we first examined phosphorylation of LKB1 and its downstream target AMPK in hearts of *Sirt3*$^{-/-}$ mice. Contrary to the findings in *Sirt1*$^{-/-}$ hearts (Fig. 5*B*), we found substantially reduced phosphorylation of LKB1 and AMPK in *Sirt3*$^{-/-}$ hearts, suggesting that activation of these targets is likely to be regulated via activation of SIRT3 (Fig. 6, *B–D*). To confirm these results, we examined the phosphorylation of LKB1 and AMPK in hearts of transgenic mice having cardiac-specific overexpression of *Sirt3*. The results showed substantially increased phosphorylation of LKB1 and AMPK in *Sirt3* transgenic hearts, thus underscoring the role of SIRT3 in activation of LKB1 and AMPK in cardiomyocytes (Fig. 6, *E–G*).

To add weight to these findings, we then tested the protein-binding and deacetylation abilities of SIRT3 to LKB1. SIRT3 was immunoprecipitated from hearts of transgenic mice and the resulting complex was tested for co-precipitation of LKB1. The results showed that SIRT3 was capable of co-precipitating LKB1 from the heart lysate (Fig. 6*H*). Next we examined the acetylation status of LKB1 in wild-type and *Sirt3*$^{-/-}$ hearts. We found increased acetylation of LKB1 in *Sirt3*$^{-/-}$ hearts, compared with wild-type controls, thus suggesting that SIRT3 was capable of associating with LKB1 and deacetylating it *in vivo* (Fig. 6*I*). To further confirm these results, we then examined the direct ability of SIRT3 to deacetylate LKB1 *in vitro*. LKB1 was immunoprecipitated from the heart lysate of a wild-type mouse, and was subjected to acetylation by PCAF or P300 *in vitro*. Our results indicated that LKB1 was preferably acetylated by PCAF (Fig. 6*J*). To test the ability of SIRT3 to deacetylate LKB1 *in vitro*, we incubated acetylated LKB1 with recombinant SIRT3 in a HDAC buffer with or without NAD. The results indicated that SIRT3 was capable of deacetylating LKB1 in a NAD-dependent manner (Fig. 6*K*).

We then tested the ability of SIRT3 to deacetylate LKB1 during hypertrophy of cardiomyocytes. Primary cultures of cardiomyocytes were overexpressed with adenovirus vectors expressing *Sirt3* wild-type or mutants and then stimulated with PE. Subsequently, cell lysate was prepared, LKB1 was immunoprecipitated and its acetylation examined by Western blotting. The results showed that acetylation of LKB1 was substantially reduced in cells where *Sirt3* wild-type, but not the mutant, was overexpressed, suggesting that SIRT3 was capable of deacetylating LKB1 *in vivo* during hypertrophy of cardiomyocytes (Fig. 6*L*).

Finally, to test whether NAD indeed requires SIRT3 to block the cardiac hypertrophic response, we examined the effect of NAD treatment in *Sirt3*$^{-/-}$ mice. *Sirt3*$^{-/-}$ mice were chronically infused with ISO, either alone or together with NAD. We found that both NAD-treated and untreated *Sirt3*$^{-/-}$ mice had a significantly increased hypertrophic response as determined by the heart weight/body weight ratio, cross-sectional area of myocytes, fibrosis of interstitial space, and expression of *Anf* and *Collagen*-α mRNA. This suggests that NAD treatment was unable to block ISO-induced hypertrophy of the *Sirt3*$^{-/-}$ heart, whereas it was capable of doing so in control hearts (Fig. 7, *A–E*). We also confirmed these results by monitoring the cardiac function of these mice by echocardiography. The LV wall thickness of wild-type mice was significantly increased after infusion of ISO, whereas it remained within control values after NAD treatment. Quantification of LV fractional shortening indicated that it was significantly reduced in wild-type mice subjected to ISO-mediated cardiac hypertrophy, but remained unchanged in NAD-treated mice, thus suggesting that NAD treatment preserved the LV function of ISO-treated wild-type mice. Evaluation of the cardiac function of *Sirt3*$^{-/-}$ mice indicated that NAD treatment was unable to prevent loss of LV function induced by ISO infusion (Fig. 7, *F* and *G*). These data thus provided strong evidence for involvement of SIRT3-mediated signaling in the anti-hypertrophic effects of NAD.

DISCUSSION

This study was designed to investigate the effects of exogenous supplementation of NAD in the development

of cardiac hypertrophy. By using different *in vitro* and *in vivo* models of hypertrophy we showed that pathologic cardiac hypertrophy is associated with depletion of cellular NAD levels. NAD treatment restored the cellular NAD levels and blocked the agonist-mediated cardiac hypertrophic response. We also identified a new substrate of SIRT3, which is LKB1. SIRT3 deacetylates LKB1, leading to activation of the kinase. Experiments carried out to demonstrate the mechanism of cardioprotective effects of NAD showed that it prevented the hypertrophic response by shutting down pro-hypertrophic Akt1 signaling, and maintaining the activity of the anti-hypertrophic AMPK signaling pathway. Another important finding in this paper is that we made a distinction between the cardioprotective effects of two sirtuin analogues that have been studied in some detail. We showed that whereas SIRT3 has the capacity to block the cardiac hypertrophic response, SIRT1 does not. These results are important from the mechanistic viewpoint of the evolution of cardiac hypertrophy as well as from the clinical standpoint for treatment of heart failure.

The role of NAD in the prevention and cure of diseases was first established in the middle of the last century, when Elvehjem *et al.* (32) showed that niacin cured pellagra in dogs. Even though NAD cured a multisymptom disease, it seemed that the therapeutic importance of this simple molecule was neglected somewhat for nearly 50 years. A few bright spots in NAD research during this time included the observation that treatment with niacin and nicotinamide can cure the porphyrinuria of liver cirrhosis, lead poisoning, and diabetes (33,–35). Although the research on the effect of exogenous NAD in preventing diseases still remains in its infancy, the significance of maintaining intracellular levels of NAD for cell protection gained momentum with the discovery of NAD-dependent deacetylases (7). The rejuvenation of the concept of NAD treatment came from studies of Araki *et al.* (36) who showed that exogenous addition of NAD to neurons delayed axonal degeneration in response to mechanical or chemical damage. Consistent with this report, Ying *et al.* (15) showed that intranasal administration of NAD profoundly decreased brain injury in a rat model of transient focal ischemia, thus highlighting the therapeutic significance of NAD. Our data supports the therapeutic value of exogenous NAD, and show for the first time that it also has the potential to block cardiac hypertrophic response.

In this study we observed substantial loss of NAD after stimulation of hearts with hypertrophic agonists, consistent with our previous studies with an aortic banding model of hypertrophy (6). In the swim-induced physiologic hypertrophy, however, no loss of NAD was detected. There could be several reasons for depletion of cellular NAD levels during pathologic hypertrophy. Stimulation of cells with hypertrophic agonists is known to induce oxidative stress, which activates poly(ADP-ribose) polymerase-1. Poly(ADP-ribose) polymerase-1 activation consumes NAD during synthesis of poly(ADP-ribose) polymers, resulting in depletion of cellular NAD levels (6). Oxidative stress is also known to induce opening of Cx43 hemi-channels, which would allow passage of molecules up to 1000 Da down to their respective concentration and electrochemical gradients (37, 38). Because the extracellular NAD concentration is lower than intracellular, opening of these channels could also contribute to loss of cellular NAD levels. There could be yet another mechanism related to the reduced activity of the NAD biosynthetic pathway, because we found reduced levels of Nampt, a key enzyme of *de novo* NAD biosynthesis, in hearts stimulated with hypertrophic agonists (28). Although relative contribution of these mechanisms for NAD loss during hypertrophy is not known at present, one would presume that all these events are occurring simultaneously leading to substantial loss of cellular NAD levels.

NAD treatment restored the cellular NAD levels and this effect was blocked by pretreatment of cells with a Cx43 channel blocker, suggesting that NAD gets entry into cells at least in part (if not all), through these channels, consistent with previous reports (21, 39). In Fig. 7*H*, we illustrated a scheme showing the sequential activation of pathways involved in NAD-mediated cardiac protection. NAD treatment was capable of maintaining the activity of AMPK. AMPK has been implicated in the activation of SIRT1 by enhancing the intracellular NAD/NADH ratio via activation of Nampt (40). Because the increased intracellular NAD/NADH ratio also activates SIRT3 (41), it is likely that stabilization of AMPK influences the activity of SIRT3 as well. In this context it should be noted that both AMPK (this study) and SIRT3 (9) are activated during physiologic

hypertrophy. The upstream kinase of AMPK is LKB1, which is known to be activated by SIRT1-mediated deacetylation in human embryonic kidney 293 cells (29). In this study, however, we found that LKB1 is activated by SIRT3 in the heart, where SIRT1 has little or no activity for this kinase. This observation is consistent with other reports in which AMPK activation in hematopoietic stem cells and neurons was found to be independent of SIRT1 (42, 43). Thus, for the cardioprotective effects of NAD, SIRT3 is upstream of LKB1, followed by AMPK. The downstream targets of AMPK included activation of Raptor and GSK3β and inhibition of Akt1 and mTOR, thereby shifting the balance of cell signaling from pro-hypertrophic toward an anti-hypertrophic pathway.

Another pathway that should be also considered involved in the anti-hypertrophic effects of NAD is the ability of NAD to reduce cellular ROS levels. Many previous studies have shown that reduction of cellular ROS levels is necessary for prevention of the cardiac hypertrophic response. Reduced cellular ROS levels after NAD treatment could be also related to activation of SIRT3. We have recently shown that SIRT3 activation induces the expression of antioxidants, Mn-SOD and catalase, by enhancing the activity of Foxo3a (9). Increased activity of antioxidants reduces cellular ROS levels, thereby blocking the activity of Ras and Ras-mediated activation of Akt1 signaling (9). These findings thus indicate that NAD treatment can block the activity of the Akt1 signaling by at least two ways, first by curtailing the cellular ROS levels by SIRT3-mediated activation of antioxidants, and second by stabilization of the activity of AMPK pathway. At any event, cardiac hypertrophy is a result of imbalance between the activity of prohypertrophic and anti-hypertrophic pathways. Based on the data presented here and published before, it seems that NAD treatment blocks the cardiac hypertrophic response by maintaining the balance between these two pathways, that is by suppressing the activity of prohypertrophic Akt1 signaling and augmenting the activity of the anti-hypertrophic AMPK-signaling pathway.

AMPK is a metabolic fuel gauge conserved along the evolutionary scale in eukaryotes that senses changes in the intracellular AMP/ATP ratio. In general, activation of AMPK boosts cellular ATP levels (44). Therefore, one would expect to see increased activation of AMPK in conditions of energy starvation. In this study, however, we found reduced activity of AMPK when cellular ATP levels were declined. This could be because the pathways leading to activation of AMPK were adversely affected by low levels of NAD during hypertrophy of cardiomyocytes. For example, decreased activity of AMPK was positively correlated with decreased activity of Nampt, which would impact intracellular levels of NAD and consequently the activity of SIRT1 and/or SIRT3 involved in activation of AMPK. Our observation that SIRT3 has the ability to activate AMPK can also explain why SIRT3-deficient hearts have defects in the ATP biosynthetic capacity (10).

The role of SIRT1 in mammalian cell growth is controversial (45,–48). This is also true regarding the mechanism of extension of the lifespan by SIRT1 (49). Although enhanced activity of Sir2 and its corresponding homologues has been shown to increase the lifespan of lower organisms such as yeast, worms, and flies, similar findings were not noted in higher organisms with SIRT1. Overexpression of SIRT1 does not extend the replicative lifespan of human fibroblasts or prostrate epithelial cells; rather, it caused replicative senescence in response to chronic cellular stress (50, 51). Also, hematopoietic stem cells obtained from SIRT1-deficient mice showed increased growth capacity and decreased dependence on growth factors (42). A similar discrepancy exists regarding the ability of SIRT1 to protect hearts during stress (8, 48). Although SIRT1 activation was shown to protect cardiac myocytes from cell death, it was never found to block the cardiac hypertrophic response. In this study, by using knock-out and transgenic mice, we found that it is SIRT3, and not SIRT1, which is responsible for transmitting the anti-hypertrophic signals of NAD. This observation is consistent with previous reports showing distinct cardiac phenotype between *Sirt3*- and *Sirt1*-deficient mice. Although *Sirt1*$^{-/-}$ mice carry cardiac developmental defects, the hearts of *Sirt3*$^{-/-}$ mice show signs of hypertrophy and fibrosis (9, 52).

In summary, we demonstrated that exogenous NAD can block cardiac hypertrophy via activation of SIRT3.

We identified a new cascade of an anti-hypertrophic signaling pathway that includes sequential activation of SIRT3-LKB1-AMPK1. Because oxidative stress is a common cause of many diseases, it is likely that many diseases are associated with depletion of cellular NAD levels. If so, then as demonstrated in this study, NAD treatment may become a panacea for prevention and cure of many diseases in the future.

Acknowledgments

We thank Drs. F. W. Alt, Harvard Medical School, Boston, and M. W. McBurney, University of Ottowa, Canada, for providing Sirt3 knock-out and Sirt1 knock-out mice, respectively. NFAT-Luc adenovirus reporter vector was provided by Dr. Jeffery Molkentin. We thank Dr. Valluvan Jeevanandam, Section Chief, Cardiothoracic Surgery, University of Chicago, for encouragement and support throughout this study.

*This work was supported, in whole or in part, by National Institutes of Health Grants RO1 HL-77788 and HL-83423.

[2]The abbreviations used are:

HDAC	histone deacetylase
AMPK	AMP-activated kinase
PE	phenylephrine
Cx43	connexin 43
Nampt	nicotinamide phosphoribosyltransferase
ISO	isoproterenol
LV	left ventricle
ROS	reactive oxygen species
Ang-II	angiotensin-II
ANF	atrial natriuretic factor
CARP	cardiac ankerin repeat protein
PCAF	p300/CREB-associated factor
CREB	cAMP-response element-binding protein
GSK	glycogen synthase kinase
mTOR	mammalian target of rapamycin
Bicine	*N*,*N*-bis(2-hydroxyethyl)glycine
CM-H_2DCFDA	5-(and 6)-chloromethyl-2,7-dichlorodihydrofluorescein diacetate
Luc	luciferase
Ac-K	acetyllysine.

REFERENCES

1. Frey N., Katus H. A., Olson E. N., Hill J. A. (2004) *Circulation* 109, 1580–1589. [PubMed: 15066961]

2. Frey N., Olson E. N. (2003) *Annu. Rev. Physiol.* 65, 45–79. [PubMed: 12524460]

3. Morisco C., Sadoshima J., Trimarco B., Arora R., Vatner D. E., Vatner S. F. (2003) *Am. J. Physiol. Heart Circ. Physiol.* 284, H1043–H1047. [PubMed: 12666659]

4. Diwan A., Dorn G. W., 2nd (2007) *Physiology* 22, 56–64. [PubMed: 17289931]

5. Sawyer D. B., Siwik D. A., Xiao L., Pimentel D. R., Singh K., Colucci W. S. (2002) *J. Mol. Cell Cardiol.* 34, 379–388. [PubMed: 11991728]

6. Pillai J. B., Isbatan A., Imai S., Gupta M. P. (2005) *J. Biol. Chem.* 280, 43121–43130. [PubMed: 16207712]

7. Haigis M. C., Guarente L. P. (2006) *Genes Dev.* 20, 2913–2921. [PubMed: 17079682]

8. Alcendor R. R., Gao S., Zhai P., Zablocki D., Holle E., Yu X., Tian B., Wagner T., Vatner S. F., Sadoshima J. (2007) *Circ. Res.* 100, 1512–1521. [PubMed: 17446436]

9. Sundaresan N. R., Gupta M., Kim G., Rajamohan S. B., Isbatan A., Gupta M. P. (2009) *J. Clin. Invest.* 119, 2758–2771. [PMCID: PMC2735933] [PubMed: 19652361]

10. Ahn B. H., Kim H. S., Song S., Lee I. H., Liu J., Vassilopoulos A., Deng C. X., Finkel T. (2008) *Proc. Natl. Acad. Sci. U.S.A.* 105, 14447–14452. [PMCID: PMC2567183] [PubMed: 18794531]

11. Bellizzi D., Rose G., Cavalcante P., Covello G., Dato S., De Rango F., Greco V., Maggiolini M., Feraco E., Mari V., Franceschi C., Passarino G., De Benedictis G. (2005) *Genomics* 85, 258–263. [PubMed: 15676284]

12. Rose G., Dato S., Altomare K., Bellizzi D., Garasto S., Greco V., Passarino G., Feraco E., Mari V., Barbi C., BonaFe M., Franceschi C., Tan Q., Boiko S., Yashin A. I., De Benedictis G. (2003) *Exp. Gerontol.* 38, 1065–1070. [PubMed: 14580859]

13. Lanza I. R., Short D. K., Short K. R., Raghavakaimal S., Basu R., Joyner M. J., McConnell J. P., Nair K. S. (2008) *Diabetes* 57, 2933–2942. [PMCID: PMC2570389] [PubMed: 18716044]

14. Lin S. J., Ford E., Haigis M., Liszt G., Guarente L. (2004) *Genes Dev.* 18, 12–16. [PMCID: PMC314267] [PubMed: 14724176]

15. Ying W., Wei G., Wang D., Wang Q., Tang X., Shi J., Zhang P., Lu H. (2007) *Front. Biosci.* 12, 2728–2734. [PubMed: 17127275]

16. Sundaresan N. R., Samant S. A., Pillai V. B., Rajamohan S. B., Gupta M. P. (2008) *Mol. Cell. Biol.* 28, 6384–6401. [PMCID: PMC2577434] [PubMed: 18710944]

17. Dong J., Sulik K. K., Chen S. Y. (2008) *Antioxid. Redox Signal.* 10, 2023–2033. [PMCID: PMC2933156] [PubMed: 18759561]

18. Jacobson E. L., Jacobson M. K. (1976) *Arch. Biochem. Biophys.* 175, 627–634. [PubMed: 8713]

19. Sugden P. H. (2003) *Circ. Res.* 93, 1179–1192. [PubMed: 14670833]

20. Sugden P. H., Clerk A. (2006) *Antioxid. Redox Signal.* 8, 2111–2124. [PubMed: 17034354]

21. Bruzzone S., Guida L., Zocchi E., Franco L., De Flora A. (2001) *FASEB J.* 15, 10–12. [PubMed: 11099492]

22. Fulco M., Cen Y., Zhao P., Hoffman E. P., McBurney M. W., Sauve A. A., Sartorelli V. (2008) *Dev. Cell.* 14, 661–673. [PMCID: PMC2431467] [PubMed: 18477450]

23. Chan A. Y., Dolinsky V. W., Soltys C. L., Viollet B., Baksh S., Light P. E., Dyck J. R. (2008) *J. Biol. Chem.* 283, 24194–24201. [PubMed: 18562309]

24. Hawley S. A., Boudeau J., Reid J. L., Mustard K. J., Udd L., Mäkelä T. P., Alessi D. R., Hardie D. G. (2003) *J. Biol.* 2, 28. [PMCID: PMC333410] [PubMed: 14511394]

25. Heineke J., Molkentin J. D. (2006) *Nat. Rev. Mol. Cell Biol.* 7, 589–600. [PubMed: 16936699]

26. Gwinn D. M., Shackelford D. B., Egan D. F., Mihaylova M. M., Mery A., Vasquez D. S., Turk B. E., Shaw R. J. (2008) *Mol. Cell.* 30, 214–226. [PMCID: PMC2674027] [PubMed: 18439900]

27. Cheng S. W., Fryer L. G., Carling D., Shepherd P. R. (2004) *J. Biol. Chem.* 279, 15719–15722. [PubMed: 14970221]

28. Imai S. I. (2009) *Cell Biochem. Biophys.* 53, 65–74. [PMCID: PMC2734380] [PubMed: 19130305]

29. Lan F., Cacicedo J. M., Ruderman N., Ido Y. (2008) *J. Biol. Chem.* 283, 27628–27635. [PMCID: PMC2562073] [PubMed: 18687677]

30. Rajamohan S. B., Pillai V. B., Gupta M., Sundaresan N. R., Birukov K. G., Samant S., Hottiger M. O., Gupta M. P. (2009) *Mol. Cell. Biol.* 29, 4116–4129. [PMCID: PMC2715814] [PubMed: 19470756]

31. Sasaki H., Asanuma H., Fujita M., Takahama H., Wakeno M., Ito S., Ogai A., Asakura M., Kim J., Minamino T., Takashima S., Sanada S., Sugimachi M., Komamura K., Mochizuki N., Kitakaze M. (2009) *Circulation* 119, 2568–2577. [PubMed: 19414638]

32. Elvehjem C. A., Madden R. J., Strong F. M., Wolley D. W. (2002) *J. Biol. Chem.* 277, e22.

33. Spies T. D., Gross E. S., Sasaki Y. (1938) *Proc. Soc. Exp. Biol. Med.* 38, 178–181.

34. Yamada K., Nonaka K., Hanafusa T., Miyazaki A., Toyoshima H., Tarui S. (1982) *Diabetes* 31, 749–753. [PubMed: 6219022]

35. Neuwahl F. J. (1943) *Lancet* 2, 348–351.

36. Araki T., Sasaki Y., Milbrandt J. (2004) *Science* 305, 1010–1013. [PubMed: 15310905]

37. Ek-Vitorín J. F., Burt J. M. (2005) *Am. J. Physiol. Cell Physiol.* 289, C1535–C1546. [PubMed: 16093281]

38. Elfgang C., Eckert R., Lichtenberg-Fraté H., Butterweck A., Traub O., Klein R. A., Hülser D. F., Willecke K. (1995) *J. Cell Biol.* 129, 805–817. [PMCID: PMC2120441] [PubMed: 7537274]

39. Bruzzone S., Franco L., Guida L., Zocchi E., Contini P., Bisso A., Usai C., De Flora A. (2001) *J. Biol. Chem.* 276, 48300–48308. [PubMed: 11602597]

40. Cantó C., Gerhart-Hines Z., Feige J. N., Lagouge M., Noriega L., Milne J. C., Elliott P. J., Puigserver P., Auwerx J. (2009) *Nature* 458, 1056–1060. [PubMed: 19262508]

41. Yang H., Yang T., Baur J. A., Perez E., Matsui T., Carmona J. J., Lamming D. W., Souza-Pinto N. C., Bohr V. A., Rosenzweig A., de Cabo R., Sauve A. A., Sinclair D. A. (2007) *Cell* 130, 1095–1107. [PubMed: 17889652]

42. Narala S. R., Allsopp R. C., Wells T. B., Zhang G., Prasad P., Coussens M. J., Rossi D. J., Weissman I. L., Vaziri H. (2008) *Mol. Biol. Cell.* 19, 1210–1219. [PMCID: PMC2262963] [PubMed: 18184747]

43. Dasgupta B., Milbrandt J. (2007) *Proc. Natl. Acad. Sci. U.S.A.* 104, 7217–7222. [PMCID: PMC1855377] [PubMed: 17438283]

44. Dyck J. R., Lopaschuk G. D. (2006) *J. Physiol.* 574, 95–112. [PMCID: PMC1817803] [PubMed: 16690706]

45. Banks A. S., Kon N., Knight C., Matsumoto M., Gutiérrez-Juárez R., Rossetti L., Gu W., Accili D. (2008) *Cell Metab.* 8, 333–341. [PubMed: 18840364]

46. Kaeberlein M. (2008) *Cell Metab.* 8, 4–5. [PubMed: 18590685]

47. Li Y., Xu W., McBurney M. W., Longo V. D. (2008) *Cell Metab.* 8, 38–48. [PMCID: PMC2822839] [PubMed: 18590691]

48. Gurd B. J., Yoshida Y., Lally J., Holloway G. P., Bonen A. (2009) *J. Physiol.* 587, 1817–1828. [PMCID: PMC2683967] [PubMed: 19237425]

49. Gan L., Mucke L. (2008) *Neuron* 58, 10–14. [PubMed: 18400158]

50. Chua K. F., Mostoslavsky R., Lombard D. B., Pang W. W., Saito S., Franco S., Kaushal D., Cheng H. L., Fischer M. R., Stokes N., Murphy M. M., Appella E., Alt F. W. (2005) *Cell Metab.* 2, 67–76. [PubMed: 16054100]

51. Michishita E., Park J. Y., Burneskis J. M., Barrett J. C., Horikawa I. (2005) *Mol. Biol. Cell.* 16, 4623–4635. [PMCID: PMC1237069] [PubMed: 16079181]

52. Cheng H. L., Mostoslavsky R., Saito S., Manis J. P., Gu Y., Patel P., Bronson R., Appella E., Alt F. W., Chua K. F. (2003) *Proc. Natl. Acad. Sci. U.S.A.* 100, 10794–10799. [PMCID: PMC196882] [PubMed: 12960381]

Figures and Tables

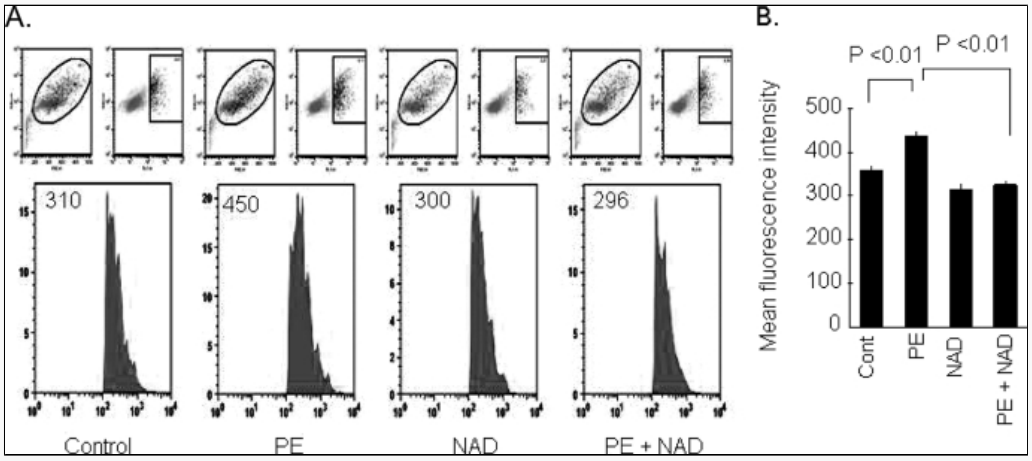

FIGURE 1.

Exogenous NAD blocks the PE-induced oxidative stress of cardiomyocytes. *A*, primary cultures of cardiomyocytes were treated with PE (20 μM) in the presence or absence of NAD (250 μM) for 15 min. Cells were stained with CM-H_2DCFDA. ROS production was measured by fluorescence-activated cell sorter. *B*, quantification of the mean fluorescence intensity in different groups of cells. Values are mean ± S.E. of five experiments.

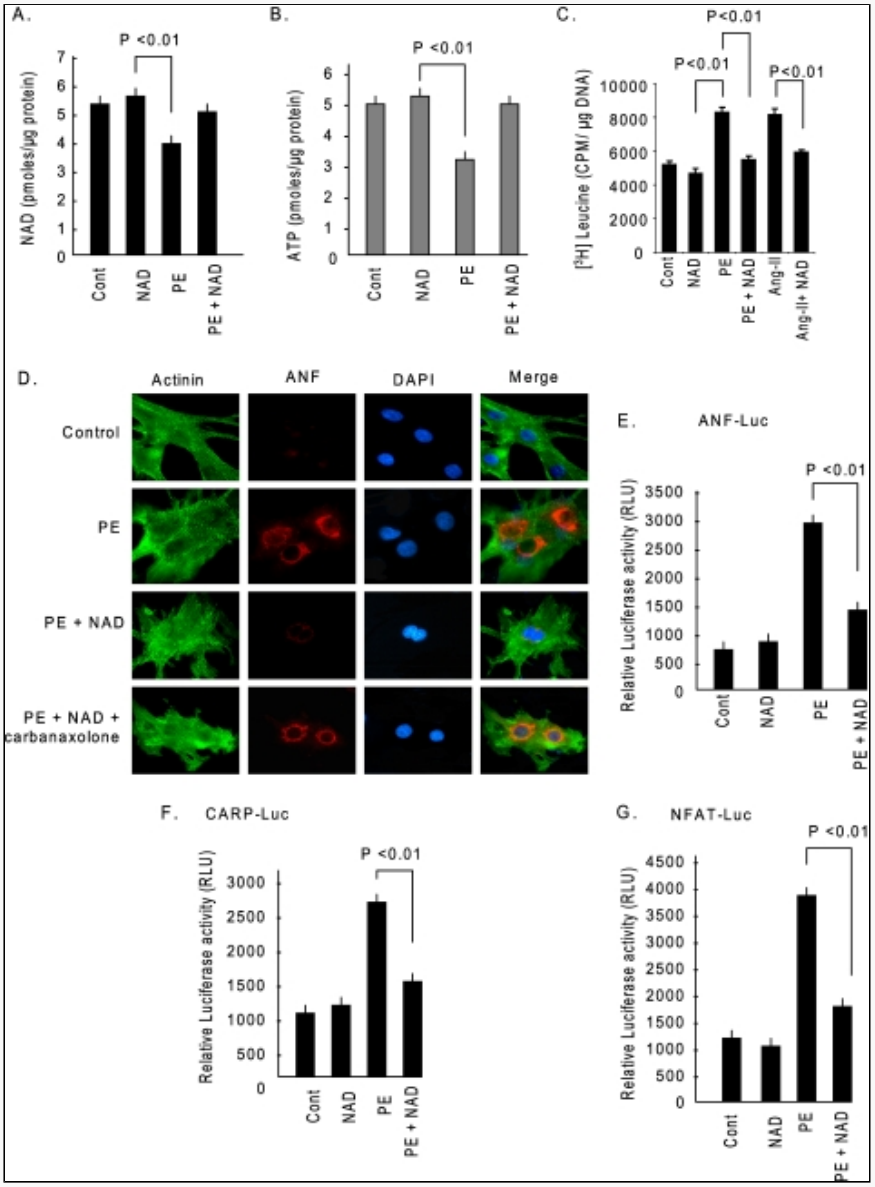

FIGURE 2.

NAD treatment blocks cardiac hypertrophic response *in vitro*. *A*, cardiomyocytes were treated with PE either alone or together with NAD. After 48 h of treatment cells were harvested and NAD content measured. *B*, ATP content was measured in the same groups of cells. *C*, cardiomyocytes were treated with PE (20 µM) or Ang-II (2 µM) in the presence or absence of NAD and labeled with [^{3}H]leucine. Forty-eight hours after treatment, cells were harvested, and [^{3}H]leucine incorporation into total cellular protein was measured. *D*, cardiomyocytes were stimulated with PE and then treated with NAD, either alone or together with carbenoxolone (10 µM). Cardiomyocytes were identified by α-actinin staining using anti-α-actinin antibody (*green*). The release of ANF from nuclei was determined by staining cells with an anti-ANF antibody (*red*). 4′,6-Diamidino-2-phenylindole (*DAPI*) stain was used to mark the position of nuclei. *E* and *F*, cardiomyocytes were transfected with luciferase reporter plasmids responsive to *ANF* (*E*) or *CARP* (*F*). Luciferase activity was measured after 8 h of treatment with PE, in the presence or absence of NAD (*G*). Cardiomyocytes were infected with a *NFAT* responsive luciferase reporter adenovirus vector. Twelve hours after infection cells were treated with PE in the presence or absence of NAD, and luciferase activity was determined 8 h post-treatment. *Cont*., control. Values presented in histograms are mean ± S.E. of six experiments.

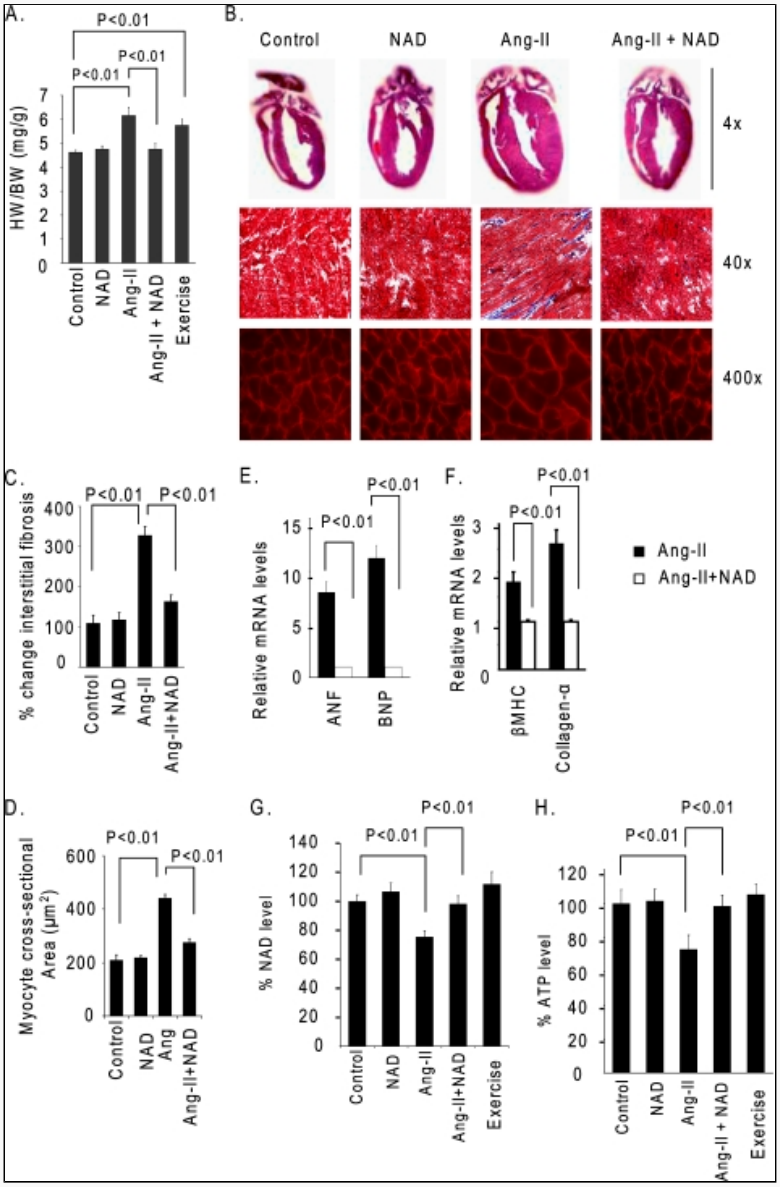

FIGURE 3.

NAD treatment blocks the agonist-induced cardiac hypertrophy *in vivo*. *A*, heart weight (*HW*)/body weight (*BW*) ratio of different groups of mice (vehicle, NAD, Ang-II, or Ang-II plus NAD-treated mice, as well as mice subjected to swim exercise). *B*, *top panel*, hematoxylin- and eosin-stained sections of whole hearts of different groups; *middle panel*, sections of hearts stained with Masson's trichrome to detect fibrosis (*blue*); *bottom panel*, heart sections stained with wheat germ agglutinin to demarcate cell boundaries. *C* and *D*, quantification of cardiac fibrosis and the myocyte cross-sectional area in different groups of mice. *E* and *F*, *Anf*, brain natiuretic peptide (*BNP*), β-myosin heavy chain (*MHC*), and *Collagen*-α mRNA levels in the heart samples of Ang-II alone or Ang-II plus NAD-treated mice. *G* and *H*, quantification of NAD and ATP contents in the heart lysate of different groups of mice as in *panel A*. Values are mean ± S.E. of five to eight experiments.

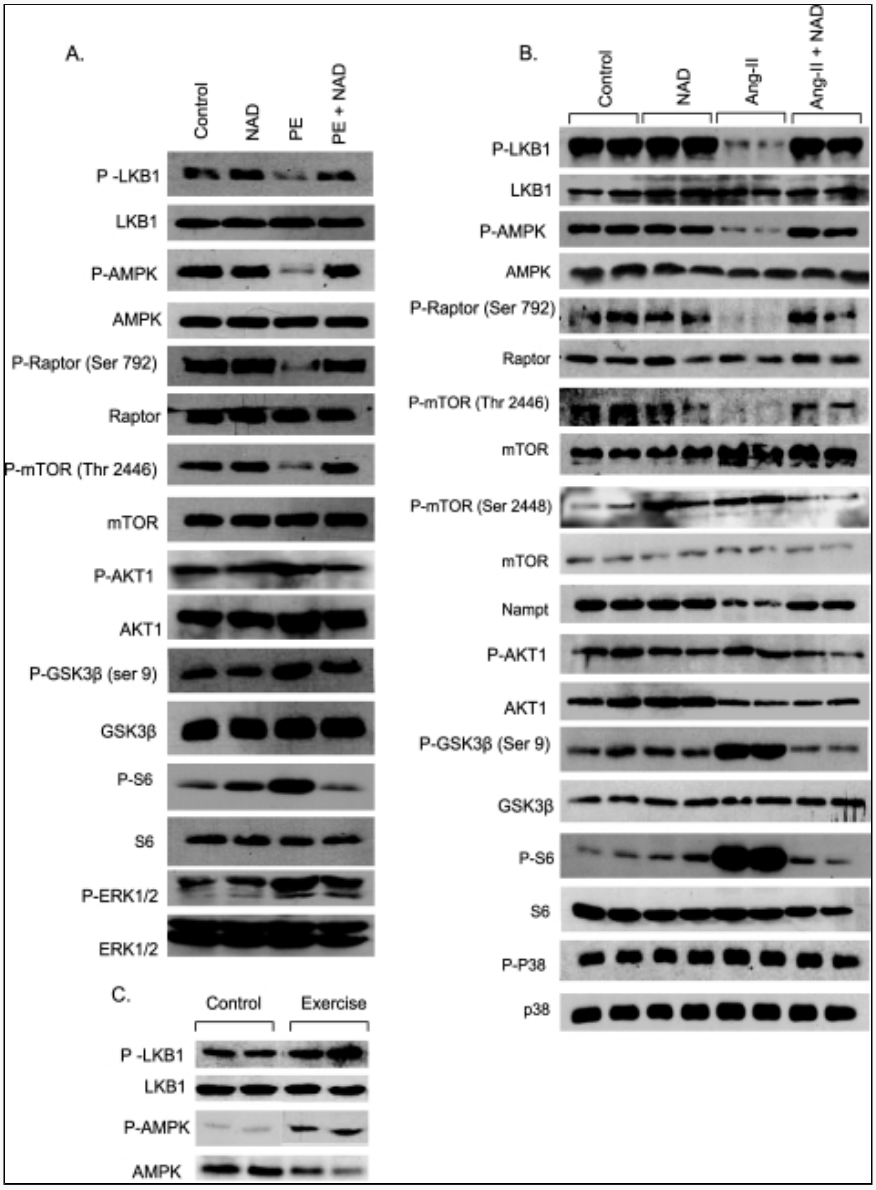

FIGURE 4.

Exogenous NAD blocks the agonist-induced signaling pathways involved in development of cardiac hypertrophy. *A*, cardiomyocytes were stimulated with PE in the presence or absence of NAD for 24 h. Cell lysate was prepared and analyzed by Western blotting with kinase-specific and phosphokinase-specific antibodies. *Numbers in parentheses* indicate the position of the phosphoamino acid recognized by the antibody. *B*, mice were treated with vehicle, NAD, Ang-II, or Ang-II plus NAD for 14 days. *C*, mice were subjected to swim exercise for 12 weeks. Heart lysate was analyzed by Western blotting with antibodies as indicated. In *panel B* and *C*, results are shown for two animals of each group.

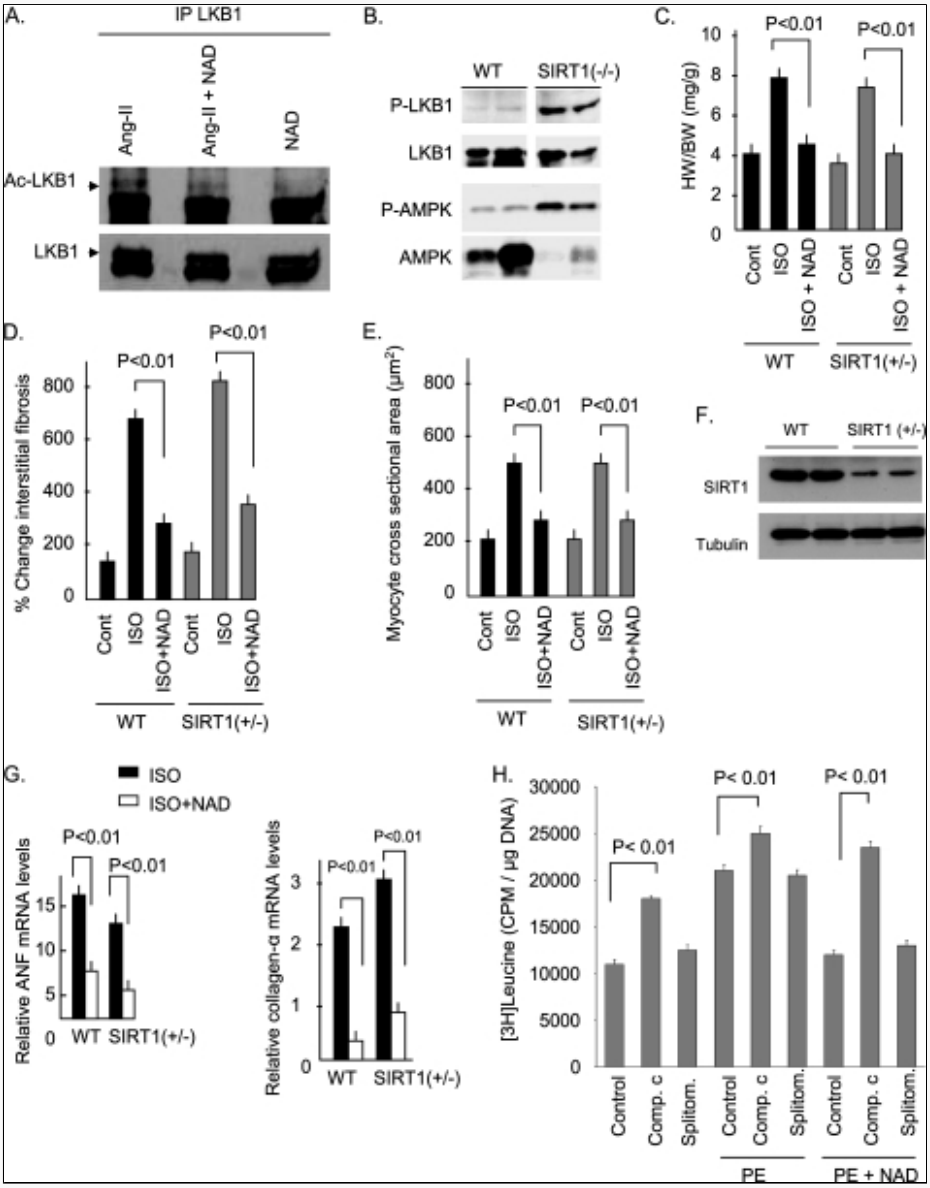

FIGURE 5.

NAD treatment blocks the agonist-mediated cardiac hypertrophy independent of SIRT1. *A*, endogenous LKB1 was immunoprecipitated (*IP*) from heart lysates of mice treated with Ang-II, Ang-II plus NAD, or NAD alone. It was analyzed by Western blotting with anti-Ac-K antibody. The stripped blot was probed with anti-LKB1 antibody for loading control. *B*, expression of phospho (*P*)-LKB1 and phospho-AMPK in the hearts of wild-type and *Sirt1*$^{-/-}$ mice. Total LKB1 and AMPK were used as loading controls. Results are shown for two mice of each group. *C*, heart weight/body weight ratio of wild-type (*WT*) and *Sirt1*$^{+/-}$ mice treated with vehicle (*cont*.) ISO or ISO plus NAD for 7 days. *D* and *E*, quantification of cardiac fibrosis and the myocyte cross-sectional area in wild-type and *Sirt1*$^{+/-}$ mice subjected to different treatments. *F*, expression levels of SIRT1 in wild-type and *Sirt1*$^{+/-}$ hearts. *G*, *Collagen*-α and *Anf* mRNA levels in heart samples of wild-type and *Sirt1*$^{+/-}$ mice subjected different treatments. *H*, primary cultures of neonatal rat cardiomyocytes were pretreated with vehicle (*control*), 20 μM compound C (*comp.c*), or 50 μM splitomicin (*splitom*.) and then stimulated with PE in the absence or presence of NAD. Cells were subsequently labeled with [^{3}H]leucine and incorporation of the isotope into total cellular proteins was measured 48 h after PE treatment. *Bar diagrams* represent values ± S.E. of five experiments.

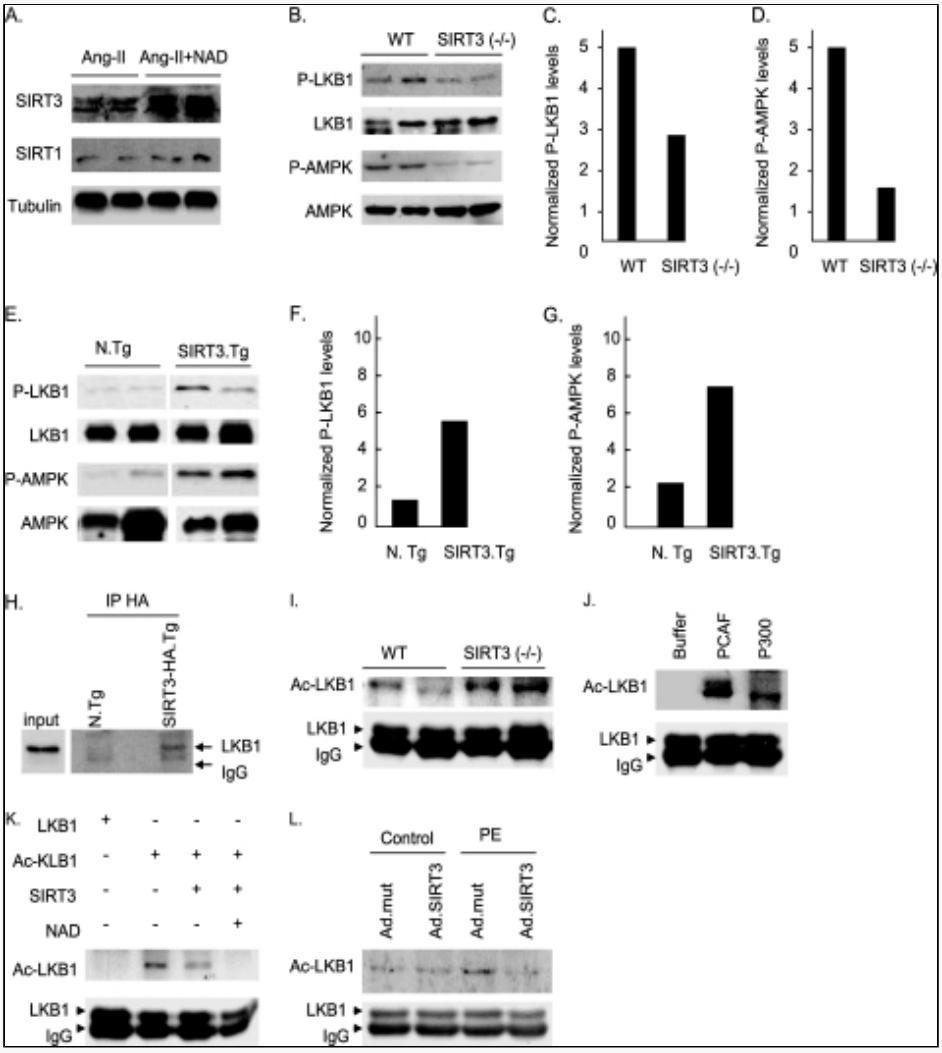

FIGURE 6.

SIRT3 binds to and deacetylates LKB1, leading to increased activity of the kinase. *A*, SIRT3 and SIRT1 expression levels in the hearts of mice treated with Ang-II, or Ang-II plus NAD. *B*, expression of phospho (*P*)-LKB1 and phospho-AMPK in the hearts of wild-type (*WT*) and *Sirt3*$^{-/-}$ mice. Total LKB1 and AMPK were used as loading controls. *C* and *D*, quantification of P-LKB1 and P-AMPK levels in the hearts of wild-type and *Sirt3*$^{-/-}$ mice. *E*, expression of phospho-LKB1 and phospho-AMPK in the hearts of non-transgenic (*N.Tg*) and *Sirt3* transgenic (*SIRT3.Tg*) mice. *F* and *G*, quantification of P-LKB1 and P-AMPK levels in the hearts of non-transgenic and *Sirt3* transgenic mice. *H*, hemagglutinin-tagged SIRT3 was immunoprecipitated (*IP*) from heart lysates of *Sirt3*·HA-Tg mice, and the resulting complex was analyzed by Western blotting with anti-LKB1 antibody. *I*, endogenous LKB1 was immunoprecipitated from heart lysates of wild-type and *Sirt3*$^{-/-}$ mice, and analyzed by Western blotting with anti-Ac-K antibody. The stripped blot was probed with anti-LKB1 antibody for loading control. *J*, LKB1 immunoprecipitated from the heart lysate of a control mouse was subjected to *in vitro* acetylation by recombinant PCAF or P300. Beads with LKB1 were separated, washed, and subjected to Western blotting with Ac-K antibody. The stripped blot was probed with anti-LKB1 antibody for loading control. *K*, LKB1 was immunoprecipitated from heart lysates and subjected to acetylation *in vitro* with PCAF. Beads containing acetylated LKB1 were then incubated with recombinant *Sirt3*, in the presence or absence of NAD. The acetylation status of LKB1 was determined by Western blotting with anti-Ac-K antibody. The stripped blots were probed with anti-LKB1 antibody for loading controls. *L*, rat cardiomyocytes were overexpressed with adenovirus vectors expressing *Sirt3* wild-type or the mutant, and treated with vehicle (control) or PE for 24 h. Cells were lysed and LKB1 was immunoprecipitated and analyzed by Western blotting with anti-Ac-K antibody. Stripped blots were probed with anti-LKB1 antibody for loading control. In *panels A*, *B*, *E*, and *I*, results are shown for two animals of each group.

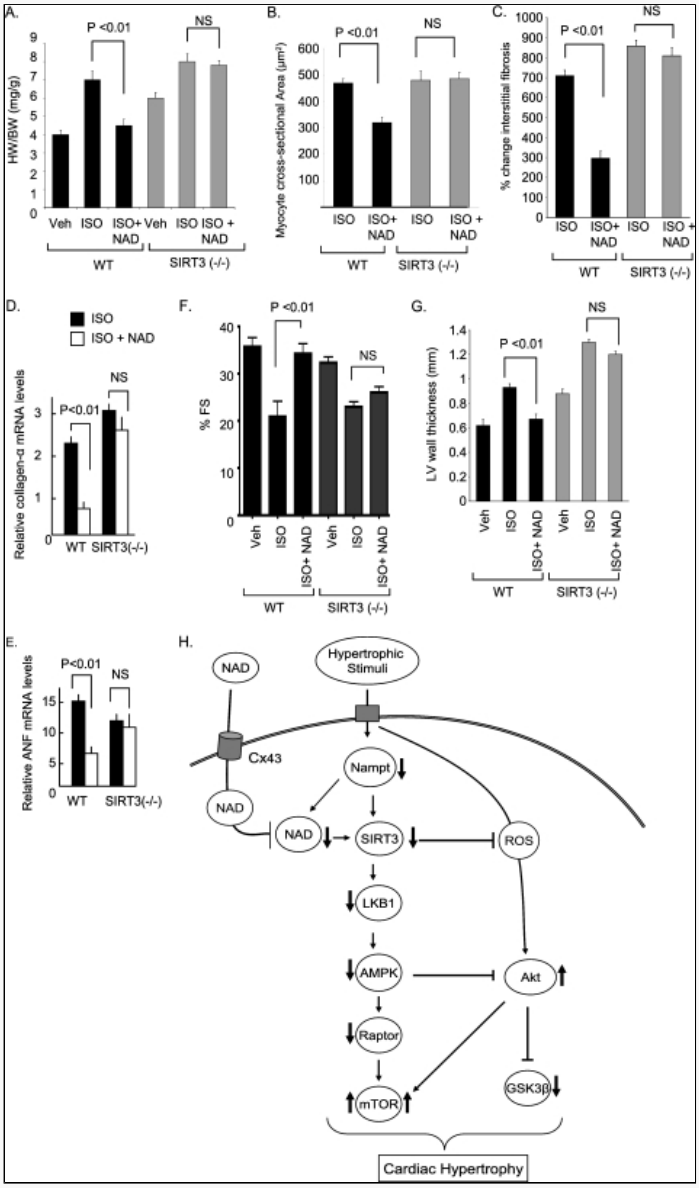

FIGURE 7.

NAD treatment is unable to block the cardiac hypertrophic response of *Sirt3*$^{-/-}$ mice. *A*, heart weight/body weight ratio of control (*Veh*), ISO, or ISO plus NAD-treated wild-type (*WT*) and *Sirt3*$^{-/-}$ mice. *B* and *C*, quantification of the cross-sectional area of myocytes and fibrosis in different groups of mice. *D* and *E*, *Collagen*-α and *Anf* mRNA levels in heart samples of WT and *Sirt3*$^{-/-}$ mice subjected to ISO-mediated hypertrophy in the presence or absence of NAD. *F* and *G*, echocardiographic measurements of LV fractional shortening and wall thickness of control (*Veh*), ISO, or ISO plus NAD-treated wild-type and *Sirt3*$^{-/-}$ mice. Values are mean ± S.E., $n = 6$. *H*, scheme illustrating signaling pathways modified by NAD to block the cardiac hypertrophic response. Stimulation of cardiomyocytes with an agonist causes reduction of cellular Nampt and NAD levels, which results in the reduced activity of SIRT3. Deceased activity of SIRT3 negatively affects the activity of the LKB1-AMPK-Raptor signaling pathway, which leads to increased activity of mTOR. Reduced activity of AMPK also regulates positively the activity of Akt1, resulting in a further activation of mTOR and suppression of the activity of GSK3β. The net result of these changes is increased protein synthesis and development of cardiac hypertrophy. Exogenous NAD enters into cardiomyocytes via connexin 43 channels, and elevates cellular NAD levels, thereby activating SIRT3. SIRT3 activation stabilizes the activity of the LKB1-AMPK signaling pathway, thus blocking the prohypertrophic activity of mTOR and of Akt1. As reported before (9), SIRT3 activation can also block cardiac hypertrophy by reducing cellular ROS levels and in so doing suppress the ROS-mediated activation of Akt1 signaling.